UNIVERSITY OF WEST BOHEMIA

Applied and Computational Mechanics 2 (2008) 123–132

Applied and Computational Mechanics

The influence of the shape of a saw-cut notch in quasi-brittle 3PB specimens on the critical applied force

S. Seitl[a,*], L. Řoutil[b], J. Klusák[a], V. Veselý[b]

[a] *Institute of Physics of Materials, Academy of Sciences of the Czech Republic, v.v.i. Žižkova 22, 616 62 Brno, Czech Republic*

[b] *Institute of Structural Mechanics, Faculty of Civil Engineering, Brno University of Technology, Veveří 331/95, 602 00 Brno, Czech Republic*

Received 3 September 2008; received in revised form 1 October 2008

Abstract

Values of fracture parameters of quasi-brittle building materials are usually determined from results of tests performed on notched testing specimens. The contribution deals with the influence of various shapes of tips of notches prepared by a diamond saw in three point bending (3PB) specimens. The influence of the notch tip shape on the applied force corresponding to a failure initiation at the notch tip and also on the critical applied force appropriate to the maximal load-bearing capacity of the specimen is studied. Calculations are performed in two finite element method (FEM) systems (ATENA, ANSYS) based on two different approaches to fracture description (Cohesive crack models and LEFM, respectively). The numerical results obtained by both FEM systems are compared. The influence of notch shapes and width is quantified.

Keywords: three point bending specimens, cement-based composites, fracture parameters, notch geometry, notch width

1. Introduction

One of the main tasks for material engineers and structural designers who deal with quasi-brittle building materials is the determination of fracture parameters. Usually these parameters are calculated from experimentally obtained data (load-deflection diagram, l-d diagram) using fracture-mechanics principles with the presumption that a stress concentrator formed in the testing specimen is a crack (e.g. [5, 10]). Then fracture mechanics for the crack as the stress concentrator with the exponent of singularity $p = 1/2$ is employed [11]. Therefore, the stress concentrator in the testing specimen should be formed into the shape that is as close to the crack as possible. It can be performed either by inserting a sharp wedge into mould during cementitious composite specimen casting and removing it after the specimen hardens, or by cutting the concentrator into a hardened plain specimen using a diamond saw or rarely a water ray. In reality, from the classical fracture mechanical point of view, any of the mentioned procedures does not create the sharp initiation crack. Both procedures provide a notched specimen, the stability of which should be evaluated by using fracture mechanics of general singular stress concentrators with the stress singularity exponent $p \neq 1/2$ (e.g. [6, 8]). This theory, however, is correct for specimens made of brittle materials.

Another possibility to study the influence of the notch shape on fracture behaviour of specimens made of cement-based composite is to use FEM simulations that employ e.g. the crack

*Corresponding author. Tel.: +420 532 290 348, e-mail: seitl@ipm.cz.

band model [2, 3]. This model belongs to the group of cohesive crack models that take into account the existence of a fracture process zone in front of the crack in cohesive materials. This group of models was proposed especially for modelling of the fracture processes in quasi-brittle materials/structures.

The paper continues in the previous studies of the influence of the notch width and the notch tip shape on fracture behaviour of the notched 3PB specimen reported recently by the authors. A double V-notch was analyzed as the first type of the notch shape employing linear elastic fracture mechanics (LEFM) in [8, 9], where particularly the influence of the notch width and length on the crack initiation and the evaluated fracture parameters were investigated (analysed by using ANSYS FEM system, ANSYS [1]). The influence of the notch width and the notch tip shape on the quasi-brittle fracture behaviour of the specimen during the fracture test was studied in [7] also by using the cohesive crack approach (ATENA FEM system [3]).

The aim of the contribution is to quantify the influence of various shapes of tips of notches in the three point bending specimens. The influence of the notch width and the notch tip shape *i*) on the applied force corresponding to the failure initiation at the notch tip and also *ii*) on the critical applied force appropriate to the maximal load-bearing capacity of the specimen is studied here. Let us note that the two load levels, i.e. *i*) and *ii*), are identical for perfectly brittle materials. For quasi-brittle materials, however, they can considerably differ.

The calculations are performed in two FEM systems (ATENA, ANSYS) based on two different approaches to fracture description (cohesive crack models and LEFM, respectively).

2. Theoretical background

The chapter is divided into two subheads. The first one covers the methodology of a generalized linear elastic fracture mechanics and a method of calculation of the critical applied force from FEM system ANSYS. The second one covers a methodological and conceptual approach of the cohesive crack models implemented in the used ATENA FEM system.

2.1. Generalized linear elastic fracture mechanics

First, the LEFM of cracks is generalized to the stress concentrators with the stress singularity exponents different from $1/2$. The assessment of such notches is based on the comparison of a controlling variable in cases of the crack and the notch [6]. As the controlling variable the mean value of tangential stress $\sigma_{\theta\theta}$ or the mean value of strain energy density factor is used within the study. It is supposed that the critical value of the controlling variable will be the same in the case of the crack initiation from the notch as in the case of the crack propagation. The results of the studies are presented in comparison of generalized stress intensity factors (GSIF) H with their critical values (generalized fracture toughness H_C) and finally by means of critical applied load.

2.2. Cohesive crack models

In this group of models the fracture process zone is represented/replaced by a fictitious crack [4] or a crack band [2], both exhibiting cohesive activity, usually decreasing with increasing crack opening. The crack band model is implemented in ATENA FEM program [3]. In this model the defined dependency between the crack opening displacement w and the crack opening stress $\sigma(w)$ is transformed according to the crack band width h. As there are four parameters available for the description of the function $\sigma(w)$ — the critical crack opening w_c, the tensile strength f_t,

the fracture energy G_f and the shape of the function — three of them are necessary for defining the function.

3. Numerical modelling

3.1. 3PB specimen with notches

The study is performed on common specimen with nominal dimensions $W \times B \times L$ equal to $100 \times 100 \times 400$ mm with span $S = 300$ mm. In the midspan of the beam the stress concentrator is created — either the crack, see Fig. 1a), or the notch. Three different types of the notch shape were analysed — the double V-notch, the $45°$ notch and the $90°$ notch (see Fig. 1b), 1c), 1d), respectively). Basic characteristics of a starting notch are its length a_n, and its width b_n. The length was $a_n = 33$ mm in all cases and the width $b_n = 0$ (for crack), 1, 2, 4 and 8 mm.

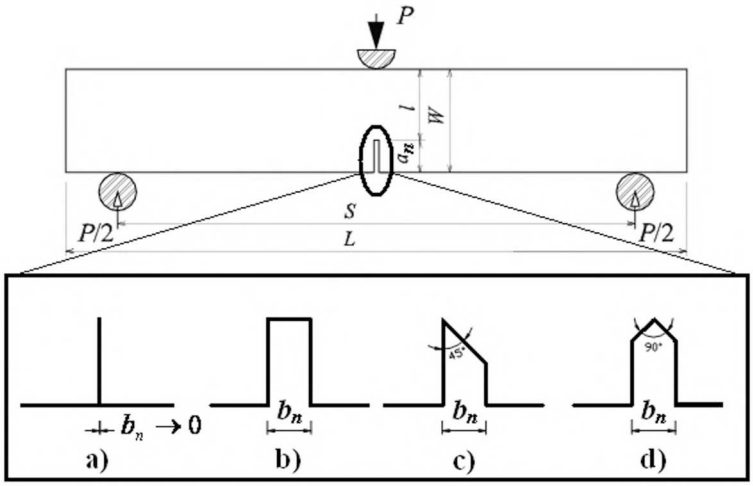

Fig. 1. Configuration of the simulated experiment — the three point bending test of the notched beam and four investigated stress concentrator shapes a) crack b) double V-notch c) $45°$ notch and d) $90°$ notch

3.2. Material parameters

The basic mechanical properties serving as input data to the used FEM codes are appropriate to a certain concrete mix tested on fracture-mechanical characteristics at Faculty of Civil Engineering, BUT Brno. The basic properties — Young's modulus $E = 44$ GPa and Poisson's ratio $\nu = 0.2$ — are complemented with the selected value of the fracture toughness $K_{IC} = 2\,\mathrm{MPa} \cdot \mathrm{m}^{1/2}$ for analyses in ANSYS and the value of the fracture energy $G_f = 280\,\mathrm{J} \cdot \mathrm{m}^{-2}$ (corresponding to the value determined from tests) for numerical simulations in ATENA. In the latter case the multi-linear tension-softening law $\sigma(w)$ was calibrated according to measured l–d diagrams with the following parameters: the tension strength $f_t = 4.7$ MPa and the critical crack opening $w_c = 0.315\,5$ mm. In both FEM systems the material is supposed to be a homogeneous continuum.

3.3. Models in ANSYS

FEM simulations in ANSYS were performed under plane strain conditions ($B = 100\,\text{mm}$) for static loading. All stresses are assumed to remain in the elastic range and the assumptions of linear elastic fracture mechanics are considered. A typical finite element mesh and boundary conditions are shown in Fig. 2. In following Figs. 3. there are shown FE meshes in the vicinity of notches and their details used for elastic simulations. The models consisted from approx. 10 000 isoparametric six or eight node elements. The typical element size near the notch tip was about $4 \times 10^{-3}\,\text{mm}$.

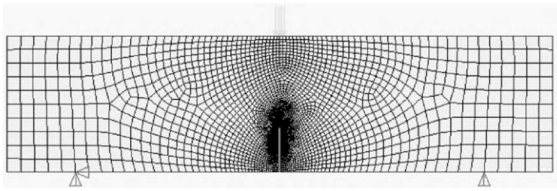

Fig. 2. Geometrical model of the specimen created in ANSYS software — the typical FE mesh and boundary conditions

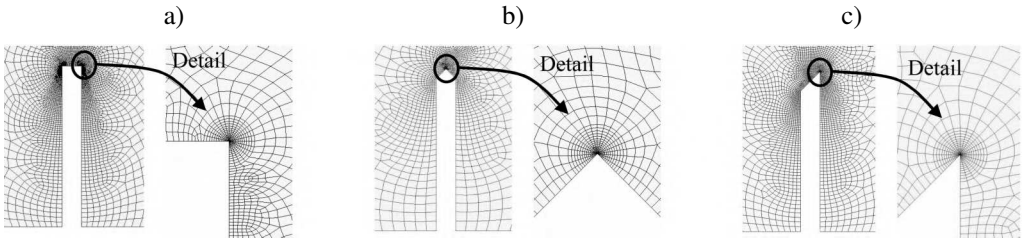

Fig. 3. The ANSYS software: FE meshes in the vicinity of notches and its details used for elastic simulations: a) 90° notch b) double V-notch c) 45° notch

3.4. Models in ATENA

FEM simulations in ATENA 2D were conducted in plain stress state with a fracture-plastic constitutive model. The fracture model is based on the classical orthotropic smeared crack formulation and the above-mentioned crack band model and it employs the Rankine failure criterion (more details in [3]). Specimens were loaded incrementally by the displacement of a testing machine jaw; the progress of the nonlinear calculation was controlled by the Newton-Raphson method. The parameters of the material model were generated to input cubic compressive strength of concrete $f_{cu} = 90\,\text{MPa}$.

A typical finite element mesh and boundary conditions are shown in Fig. 4. Central parts of the performed models were covered by the FE mesh of the defined finite element size $e = \{1, 2, 4\}\,\text{mm}$ (see Fig. 5). A considerably more rough mesh was created out of the region where the number of finite elements along the specimen depth was set to 8 (due to cut on computational costs). Several FE mesh densities in the central part of the model were taken into account in order to diminish the possible influence of the finite element size and shape on the simulated fracture behaviour which can arise from the character of the smeared crack approach implemented in ATENA.

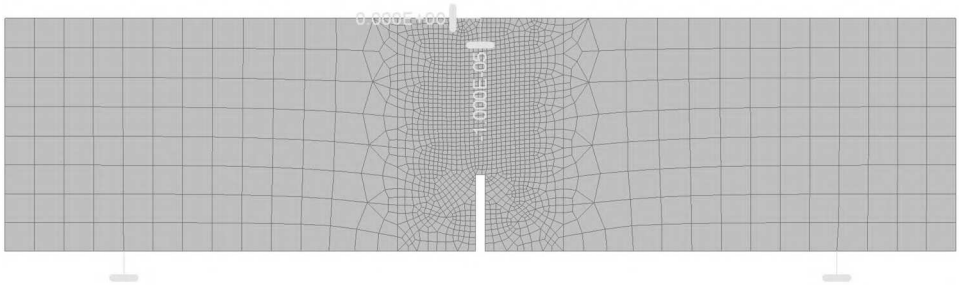

Fig. 4. Geometrical model of the specimen created in ATENA software — the typical FE mesh and boundary conditions

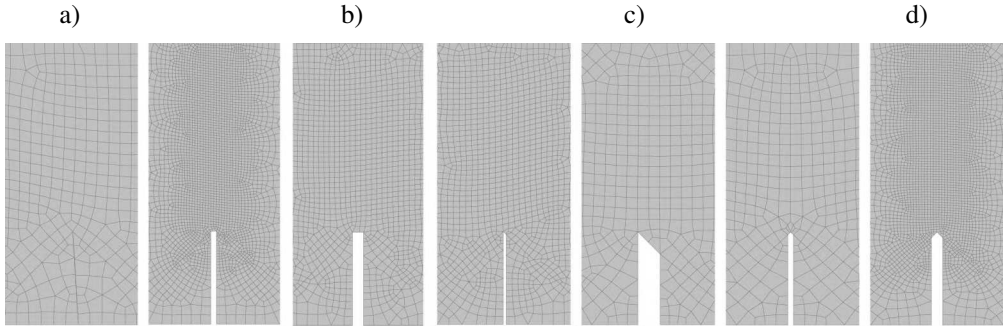

Fig. 5. Details of some of the FE meshes used for the simulations performed by ATENA software: a) crack, b) double V-notch, c) 45° notch, d) 90° notch

4. Results and discussion

The results of the calculations are divided into three parts. In the first two subsections the numerical results from ANSYS and ATENA, respectively, are introduced, the last one covers the comparison of both sets of results obtained by the mentioned FEM systems.

4.1. Results from ANSYS

The numerical studies were performed for the loading force $P = 800\,\text{N}$.

Curves of an initiation angle are shown in Fig. 6a). It is obvious that the initiation angles for the crack and for the 90° symmetrical notch are zero. It means that only a normal mode occurs there. The 45° notch and the double notch have the non-zero crack initiation angle that means the crack initiation in a mixed-mode (normal and shear modes).

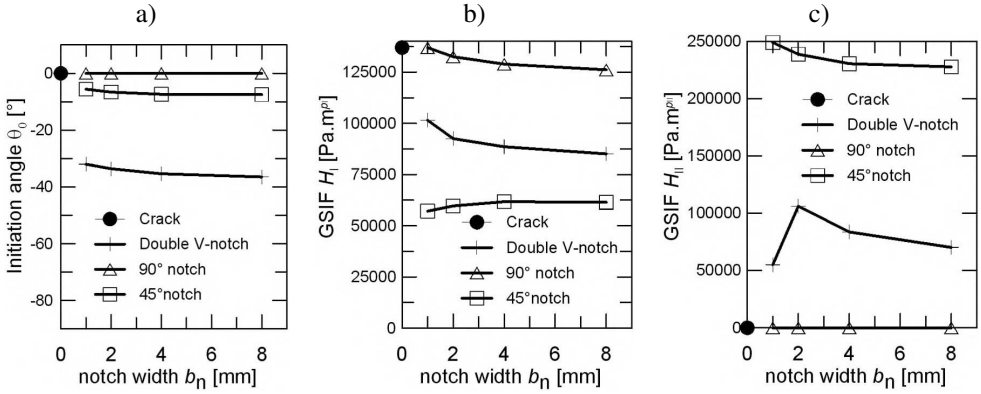

Fig. 6. a) The crack initiation angle $\tilde{\theta}_0$, b) the curves of the generalised stress intensity factor H_I, c) the curves of the generalised stress intensity factor H_{II}; GISF values are for $P = 800\,\mathrm{N}$

The curve's shapes of the general stress intensity factor for the stress concentrators (shown in Ch 3.1.) are shown in Fig. 6b), 6c). The units of the general stress intensity factors H_I and H_{II} are $\mathrm{Pa} \cdot \mathrm{m}^{pI}$ and $\mathrm{Pa} \cdot \mathrm{m}^{pII}$ respectively. The stress singularity exponents for the studied concentrators are: a) crack $p_I = 0.5$, $p_{II} = 0.5$, b) double V-notch $p_I = 0.455\,5$, $p_{II} = 0.091\,5$, c) $90°$ notch $p_I = 0.455\,5$, $p_{II} = 0.091\,5$, and d) $45°$ notch $p_I = 0.474\,6$, $p_{II} = 0.300\,7$.

Note that in Figs. 6–7. the black point on the vertical axe corresponding to the zero notch width holds for a crack.

The crack initiates in the mixed mode, but the normal mode is dominant and the comparison of H_I with its critical value H_{CI} suffices. Furthermore the ratio of the normal and shear modes is included in the stability criteria [6]. The critical value H_{IC} is shown in Fig. 7a).

As it is not possible to compare the values H_{IC} mutually for the notches with varying exponents p_I, due to varying units, the critical applied force is used for better understanding of numerical results, see below.

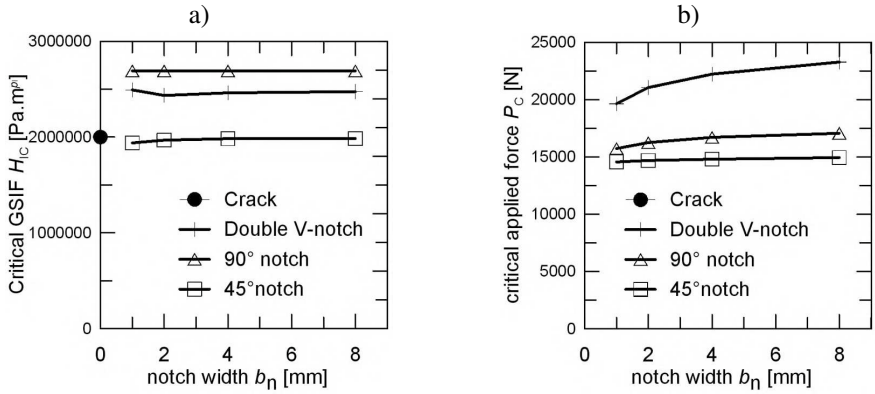

Fig. 7. a) The value of critical GSIF, b) the value of the critical applied force P_C versus the notch width b_n

The values of the critical applied force for the studied concentrators with the material parameters specified in the chapter 3.2. in the case of the three point-bend tests are presented in Fig. 7b). The strongest stress concentrator is of course the crack — the critical force for the crack growth is the lowest. If the notch is used the critical applied force will be greater in the

dependence on the notch shape. The dependence on the notch width b_n for a separate shape is negligible.

4.2. Results from ATENA

A typical output of a loading test on the quasi-brittle specimen, the virtual one as well, is a recorded dependence of the force by which the tested specimen resists the applied displacement (l–d diagram). From such a record specific points, parts or even the whole curve is used for the determination of the fracture parameters of the quasi-brittle materials. Simulated l–d diagrams for selected versions of FE mesh of models of 3PB beams with the crack, individually studied notch tips and selected notch widths are depicted in Fig. 8. Loading curves for the other variants of FE meshes can be found in [7]. It is evident from this picture that the influence of the stress concentrator on the structural behaviour of the quasi-brittle specimen is not significant and the small variations of the l–d (applied force versus midspan deflection) curves are caused mainly by the variations of the FE mesh formation around the notch tip.

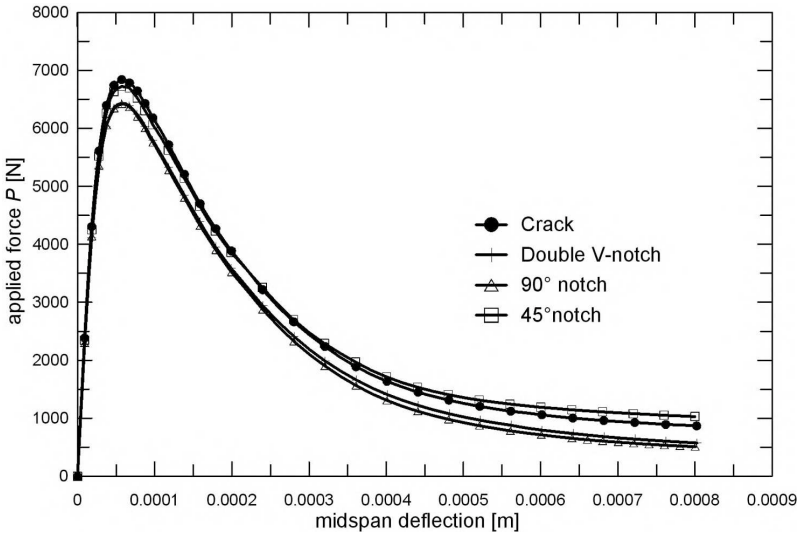

Fig. 8. Simulated load–deflection diagrams for the 3PB test on beams with crack, double V-notch, $90°$ notch, $45°$ notch — versions with the FE mesh with the element size $e = 2\,\text{mm}$ and the notch width $b_n = 4\,\text{mm}$

The critical applied forces P_u from these analyses, i.e. peak loads from the recorded l–d diagrams, are compared in Fig. 9. It can be seen, contrary to the results presented in the preceding section, that the value of P_u stays more or less constant with the changing notch width regardless to the notch tip shape.

The applied force which corresponds to the further crack propagation from a pre-existing crack or to the crack initiation from a notch, respectively, could not be obtained directly from the results of the performed calculations. The value of the crack initiation force P_{ini} was therefore determined from an extrapolation of the dependence of the applied force versus the crack width from loading steps at the initial stage of the fracture. Values of both, the applied force P and the crack width w (i.e. the crack opening displacement COD), were extracted from the results of the numerical simulations at several loading steps after the loading step when the failure at the

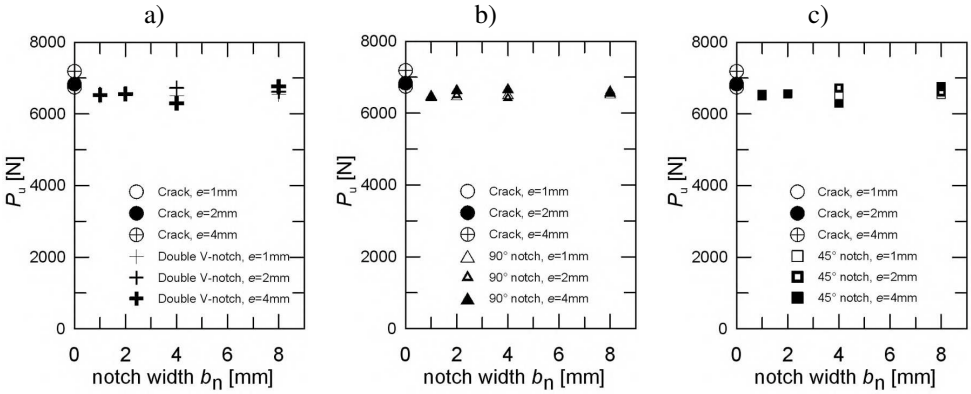

Fig. 9. The value of the critical (ultimate) applied force P_u versus the notch width b_n for a) crack and double V-notch, b) crack and 90° notch, c) crack and 45° notch

initial crack/notch tip was indicated (see Fig. 10 left). Then the extrapolation of the dependence using a low order polynomial function was performed to estimate the applied force at the crack initiation, i.e. at $w = 0$ (see Fig. 10 right).

As the shapes of the finite elements at the initial crack/notch tip differ for the individual analysis, which is the reason for slight differences of the directions of crack created in these elements during loading (Fig. 10), a specific procedure had to be used for the determination of the crack opening of the smeared crack propagated from the individual studied stress concentrators. A sum of the projections of crack openings in the individual finite elements neighbouring the stress concentrator tip was assumed as the crack width w.

The dependence of the crack initiation force P_{ini} on the notch width and the notch tip shape, together with its comparison to the situation with the pre-existing crack is depicted in Fig. 11.

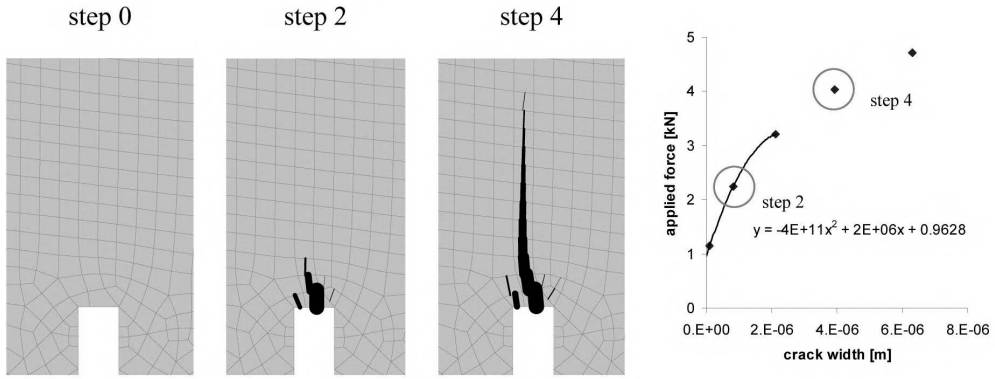

Fig. 10. The illustration of the procedure used for the determination of the crack initiation force P_{ini}

4.3. Discussion and comparison of results

In this paragraph the numerical results obtained by both FEM systems are discussed and compared. Since the slightly different values of material constants were used as input data for

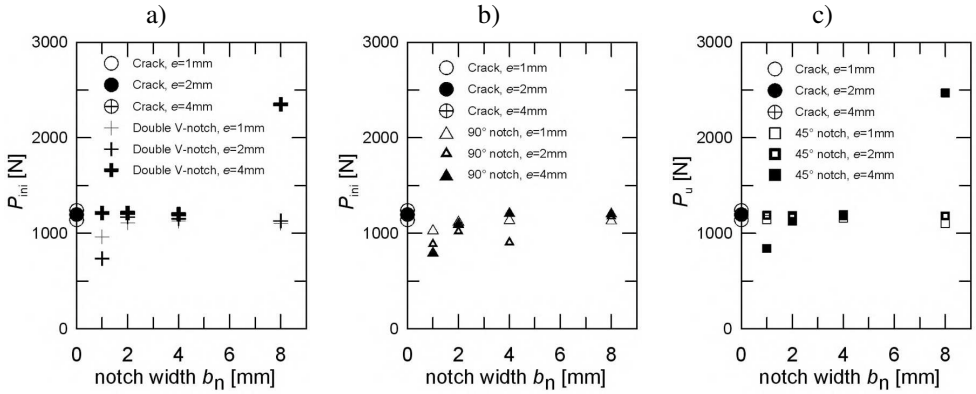

Fig. 11. The value of the applied force P_{ini} versus the notch width b_n for a) crack and double V-notch, b) crack and 90° notch, c) crack and 45° notch

studies in ANSYS and ATENA, see chapter 3.2., normalised values of the limit loading forces $P_{x,N}$, where $x = \{C, \mathrm{ini}, u\}$, were defined as ratios $P_{x,N} = P_x(\mathrm{notch})/P_x(\mathrm{crack})$.

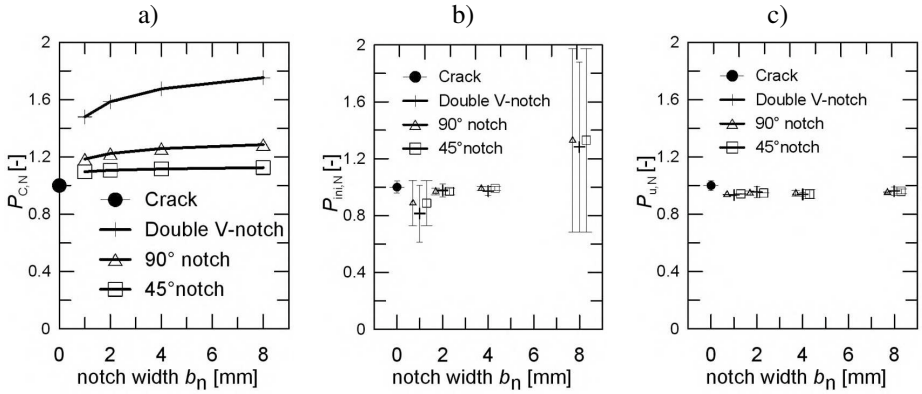

Fig. 12. The comparison of a) the normalized critical applied force versus the notch width b_n for different notch tip shapes (brittle material), b) the normalized crack initiation force $P_{\mathrm{ini},N}$ versus the notch width b_n for different notch tip shapes (the quasi-brittle material), c) the normalized ultimate force $P_{u,N}$ versus the notch width b_n for different notch tip shapes (the quasi-brittle material)

In Fig. 12 the normalized critical applied force $P_{C,N}$ (in the case of the brittle material), the crack initiation force $P_{\mathrm{ini},N}$ and the ultimate force $P_{u,N}$ (both for the quasi-brittle material) are plotted for different notch tip shapes as the function of the notch width. In the case of the quasi-brittle material the graphs b) and c) show the mean value $\pm$standard deviation from the results calculated for all considered FE meshes, see [7]. We can see that the different approaches have different results for studied concentrators. In case of use of the generalized fracture mechanics (brittle material): the value of the normalised critical force $P_{C,N}$ slightly grows up with the notch width (especially for the double V-notch) and is generally higher for the notches with weaker singularities, see Fig. 12a). When the theory of the cohesive crack model is used (the quasi-brittle material): the normalised forces $P_{\mathrm{ini},N}$ and $P_{u,N}$ does not depend on the shape and width of the stress concentrators, see Figs. 12b) and 12c).

5. Conclusion

The influence of the starting notch geometry on the fracture behaviour of the three point bend specimen has been investigated in this paper by using FEM systems ANSYS and ATENA. The corresponding numerical models based on finite element method simulations have been suggested and the dependence of the fracture behaviour of the specimen on the starting notch widths was shown.

The results obtained are summarised in the following paragraph:

1. In case of use of the generalized fracture mechanics: the normalised critical force slightly grows up with the notch width and is generally higher for the notches with weaker singularities.
2. When the theory of the cohesive crack model is used the normalised initiation and ultimate forces do not depend on the shape and width of the stress concentrators.
3. The quantification of the notch width and the notch tip shape influence on the fracture parameters determined from the tests on specimens made of silicate based materials that lie on the transition between the brittle and the quasi-brittle failure manner (e.g. cement pastes, mortars or fine concretes) stays unresolved as a challenge for the future research.

Acknowledgements

The work has been supported by the grant project 103/07/1276 and by the research project of Academy of Sciences of the Czech Republic No. AVOZ 20410507.

References

[1] ANSYS Users Manual Version 10.0, Swanson Analysis System, Inc., Houston, Pennsylvania, 2005.
[2] Z. P. Bažant, B. H. Oh, Crack band theory for fracture of concrete. Materials and Structures 16 (3) (1983) 155–177.
[3] V. Červenka, et al, ATENA Documentation. Cervenka Consulting, Prague, 2005.
[4] A. Hillerborg, M. Modéer, P. E. Petersson, Analysis of crack formation and crack growth in concrete by means of fracture mechanics and finite elements. Cement and Concrete Research 6 (1976) 773–782.
[5] B. L. Karihaloo, Fracture mechanics of concrete. Longman Scientific & Technical, New York, 1995.
[6] J. Klusák, Z. Knésl, L. Náhlík, Crack initiation criteria for singular stress concentrations, Part II: Stability of sharp and bi-material notches. Engineering mechanics 14 (6) (2008).
[7] L. Řoutil, V. Veselý, Influence of notch shape and width on load-deflection diagram/fracture parameters of cement based composite, Engineering mechanics 2008, Svratka, Czech Republic (2008) 796–806.
[8] S. Seitl, J. Klusák, Z. Keršner, The influence of a notch width on a crack growth for various configurations of three-point bending specimens. Materials Engineering 14 (3) (2007) 213–219 (in Czech).
[9] S. Seitl, J. Klusák, Z. Keršner, Influence of notch width and length on crack initiation in 3PB specimens, Engineering mechanics 2008, Svratka, Czech Republic, (2008), 807–811.
[10] S. P. Shah, S. E. Swartz, Ch. Ouyang, Fracture mechanics of structural concrete: applications of fracture mechanics to concrete, rock, and other quasi-brittle materials, John Wiley & Sons, Inc., New York, 1995.
[11] M. L. Williams, On the Stress Distribution at the Base of Stationary Crack, Journal of Applied Mechanics 24 (1957) 109–114.